Journal of Fashion Business
Vol. 8, No. 6, pp.68~77(2004)

Characterization of Luster Properties of Nylon 6 Hollow Filament Yarn Woven Fabric

- Three-dimensional Simulation of Hollow Filament -

Kim, Jong-Jun*, Jeon, Dong-Won and Jeon, Jee-Hae*****

Prof., Dept. of Clothing and Textiles, Ewha Womans University*
Prof., Dept. of Clothing and Textiles, Ewha Womans University**
Graduate Student, Dept of Clothing and Textiles, Ewha Womans University***

Abstract

Hollow filament yarns provide better warmth to the touch, lighter in weight, increased opacity, and subtle luster compared to the regular synthetic filament yarns. However, luster properties of textile fibers or fabrics are often difficult to characterize, partly due to the fineness of the surface texture, the anisotropic nature of the weave structure, the complexity of the fiber array comprising a yarn, and the fiber structure itself. In this study, the fabric surface luster image was analyzed using image analysis methods after image acquisition. The hollow filament fiber was modeled using a three-dimensional modeling software. It was then ray-traced for comparing the virtual luster images of the hollow fiber and the regular fiber models based on shading models including photon mapping. The luster object size of the actual hollow filament fabric was smaller than that of the regular filament fabric. The shape of the luster object of the hollow filament fabric was dual peak type while that of the regular filament was single.

Key words: Hollow Filament, Nylon 6, Luster, Three-dimensional Modeling

I. Introduction

Continuous hollow filament yarns may provide advantages such as increased cover or opacity, lighter weight fabrics, better insulation, warmness to the touch, a dry hand which enhances the body and drape characteristics of fabrics made using fine filament yarns due to the inner void.[1)] The manufacture of the hollow filament yarn needs void content control, since the void may collapse during the melt spinning of the polymer or the drawing/twisting process. It has long been desirable to provide undrawn hollow filaments for which there is essentially no loss in void content (VC) on drawing. Since the melt spinning of hollow fiber using a special spinneret needs also more precise control of the quenching air temperature and/or flow profile for the inner void not to collapse due to the melt viscosity fluctuation or the cooling condition perturbation. It is desirable that any new polyester filaments should have a capability to be partially or fully drawable with or without heat or without post heat-treatment to uniform filaments.

With the advancement in the computer based modeling and simulation sectors, virtual fibers,

yarns, woven fabrics, knitted fabrics modeling and rendering have been reported recent yeras. [2] One may generate a filament fiber or yarn based on a sweeping curve. The basic idea of the generative model is to create each yarn by sweeping a closed curve along a centerline path. The closed curve and centerline path represent cross-sectional shape and the centerline configurations of the constituent yarns, respectively.[3] With this kind of centerline curve, one can define a unique plane through any point on the centerline curve which is perpendicular to the centerline curve. In this study, the curves of yarn cross-section and yarn centerline were constructed into a three-dimensional object to represent the filament.

Due to the refraction and scattering by the canals or voids, the hollow yarns exhibit rather subdued luster characteristics compared to the non-hollow regular filaments. In order to characterize the subtle luster properties of the hollow filament yarn, a nylon 6 hollow filament yarn fabric and a regular nylon 6 filament yarn fabric were compared using the image analysis[4] of the acquired images of the fabric or yarn surface. Virtual three dimensional modeling[5] and the ray-tracing and photon mapping techniques were employed to better understand the luster characteristics of the hollow filament yarns.

II. Theoretical Backgrounds

When we consider the luster characteristics of a filament or a fabric, it is needed to review the definition of the reflection models. Reflection is the process by which light incident on a surface interacts with the surface in such a way that it leaves on the incident side without change in frequency.[6] The properties involved in it are spectra, polarization, and directional distribution. A reflectance is a ratio of reflected power to incident power. One of the reflection models is the Phong model[7] which is an empirical model based on physical observation, which used a term for specular reflectio^n, α, where n normally has the value range of 1 to a few hundreds. Therefore the model is not physically accurate even if it is easy to simulate or calculate. When we focus on the polymeric materials, they may be regarded as dielectric media.

For dielectric materials of non-absorbing with smooth surfaces and no disturbing surface layers, the Fresnel equations[6] become

$$r_p = \frac{\tan(\theta_i - \theta_t)}{\tan(\theta_i + \theta_t)} \tag{1}$$

in the case of *P* polarized light, and

$$r_s = \frac{\sin(\theta_t - \theta_i)}{\sin(\theta_t + \theta_i)} \tag{2}$$

in the case of *S* polarized light, where θ_i = angle of incidence, and θ_t = angle of transmission.

For unpolarized light, the total Fresnel reflectance becomes as below:

$$F_r = \frac{1}{2}(r_p^2 + r_s^2) \tag{3}$$

The Whitted shading model[8] is a shading model which models the effects of ambient illumination, direct diffuse illumination from sources, direct specular illumination from sources, refraction and reflection.

$$I_\lambda = I_{a\lambda}k_aO_{d\lambda} + \sum_{1\le i\le m} S_i f_{att} I_{p\lambda}\left[k_dO_{d\lambda}(\overline{N}\cdot\overline{L}_i) + k_s(\overline{N}\cdot\overline{H}_i)^n\right] + k_sI_{r\lambda} + k_tI_{t\lambda} \tag{4}$$

$I_{r\lambda}$ and $I_{t\lambda}$: reflected intensity and refracted intensity,
k_t: transmission coefficient,
S_i: coefficient for occlusion,
f_{att}: light source attenuation factor,

$O_{d\lambda}$: diffuse reflection color,
$\overline{N}$: surface normal vector,
$\overline{L}$: light direction vector,
$\overline{H}$: halfway vector.

The photon mapping is capable of simulating the refraction of light through a transparent substance, reflections between illuminated objects, and some of the effects caused by particulate matter.[9] In the context of the refraction of light through a transparent medium, the desired effects are called caustics. A caustic is a pattern of light that is focused on a surface after having had the original path of light rays bent by an intermediate surface. With photon mapping light packets (photons) are sent out into the scene from the light source and whenever they intersect with a surface, the three dimensional coordinate of the intersection is stored in the cache, also called the photon map, as well as the incoming direction and the energy of the photon. As each photon is bounced or refracted by intermediate surfaces, the energy gets absorbed until no more is left. We can then stop tracing the path of the photon. This is generally a pre-process and is carried out before the main rendering of the image. Often the photon map is stored on disk for later use. Once the actual rendering is started, every intersection of an object by a ray is tested to see if it is within a certain range of one or more stored photons and if so, the energy of the photons is added to the energy calculated using a more common equation.

The rendering equation can be expressed as follows:[9]

$$L_r = \int_{\Omega} f_r L_{i,l} \cos\theta_i d\omega_i + \int_{\Omega} f_{r,s}(L_{i,c} + L_{i,d}) \cos\theta_i d\omega_i + \int_{\Omega} f_{r,d} L_{i,c} \cos\theta_i d\omega_i + \int_{\Omega} f_{r,d} L_{i,d} \cos\theta_i d\omega_i + \quad (5)$$

where

$$f_r = f_{r,s} + f_{r,d} \text{ and } L_i = L_{i,l} + L_{i,c} + L_{i,d}$$

In this equation the incoming radiance has been split into contributions from the light sources, contributions from the light sources via specular reflection (caustics), and indirect soft illumination.

The diffuse part represents all reflection models from Lambertian to slightly glossy while the specular part is highly glossy and ideal specular reflection models. The first pass in the method is constructing the photon map by emitting photons from the light sources in the model and storing these in the photon map as they hit surfaces. The final image is rendered using Monte Carlo ray tracing[9] in which the pixel radiance is computed by averaging a number of sample estimates. Each sample consists of tracing a ray from the eye through the pixel into the target scene.

III. Experiments

1. Fabric Specimens

As a control specimen, nylon 6 regular, non-hollow, filament fabric, nominal denier of 210d was used. As a hollow filament fabric, nylon 6 hollow, with square shape, filament fabric, with nominal denier of 210d and actual denier of 180d was used<Table 1>.

2. Image Acquisition

A color CCD(charge coupled device) camera

<Table 1> Fabric and yarn specifications

Specification	Hollow Filament Fabric	Regular Filament Fabric
Denier/Filament	210d/34f	210d/34f
Fiber Void Content, %	16	0
Fabric Thickness, mm	0.208	0.151

with 2080 × 1542 pixels of interline transfer image sensor was used for the fabric image acquisition. It has a typical dynamic range of 61dB. Under normal image acquisition practice, the photon receptors of the CCD usually collect a large number of photons from the luster objects area of the sample fabric. Therefore, we may well employ a CCD camera with a high dynamic range. A trinocular microscope was used for the CCD camera mounting.

3. Image Processing and Analysis

As an image processing and analysis program, a public-domain JAVA software called the ImageJ (National Institute of Health, USA) was used. With this one can handle 8-bit, 16-bit and 32-bit images. It is possible to measure distances and angles. A built-in function of three-dimensional representation of the image pixel values is also used to visually compare the luster area of the fabric images. It supports standard image processing functions such as contrast manipulation, sharpening, smoothing, edge detection and median filtering. After acquisition of the fabric image, the *Threshold* function was used to select luster objects on the filament fabric image. Then the *Analyze Particle* function was selected to calculate the area of the luster objects ('blobs'). This command counts and measures objects in binary or thresholded images. It works by scanning the image or selection until it finds the edge of an object. It then outlines the object using the wand tool, measures it using the *Measure* command, fills it to make it invisible, then resumes scanning until it reaches the end of the image or selection. Particles smaller than *Minimum Size*, in this case, 100 pixels, were ignored. Outlines of the measured particles or blobs were recorded as TIFF. The sum and average values of the luster objects on the fabric specimens were calculated.

4. Virtual Modeling of the Hollow Filament Fiber

In order to investigate the luster properties of a hollow filament fiber model, a three-dimensional modeling program, Rhinoceros3D (McNeel and Associates, USA), was used. Since the void content of the actual hollow filament was 16%, the square hollow section dimension was calculated accordingly. A cylindrical solid model was first prepared, and square cross-section bar was subtracted from the first cylindrical solid by using the CSG(constructive solid geometry) method. The solid was assumed to have a refractive index of 1.53 for the nylon 6 fibrous material. The values of the fade_color (R,G,B) were 0.5, 0.8, and 0.6, respectively. Two point light sources were positioned over the virtual hollow filament fiber model. In order to verify the effect of photon mapping and the caustics, a solid plate, with gray color of 0.41, was positioned below close to the model.

IV. Results and Discussion

1. Modeling and Ray-tracing

The propagation of the incident ray was schematically presented in <Fig. 1>. The virtual

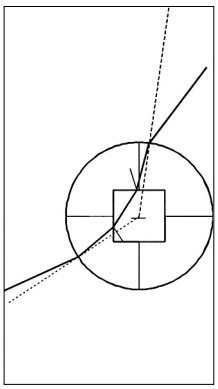

<Fig. 1> Schematic representation of the propagation of an incident ray through the cross section of a hollow nylon filament fiber

hollow fiber model was assumed to have air in the square canal. The ray is refracted mostly, in the specific case of this schematic, toward the center of the cylinder first, and some portion of the incident ray was reflected at an angle of reflection. Some of the ray was again refracted, reflected, absorbed, or scattered inside.

Three dimensional virtual model was prepared using a modeling software to simulate the hollow filament as shown in <Fig. 2>. In order to verify the effect of photon mapping, a base plate with gray color was positioned underneath of the hollow fiber model.

As shown in<Fig. 3a, 3b>, the non-hollow fiber cylinder reflects more of incoming light and its caustics by the photon gathering on the base plate are more evident. From this virtual model, it is concluded that the reflection intensity and the caustics intensity are higher for the regular fiber model, and those for the hollow filament model are lower. This results in the subdued reflection from the hollow fiber. If the fiber models are

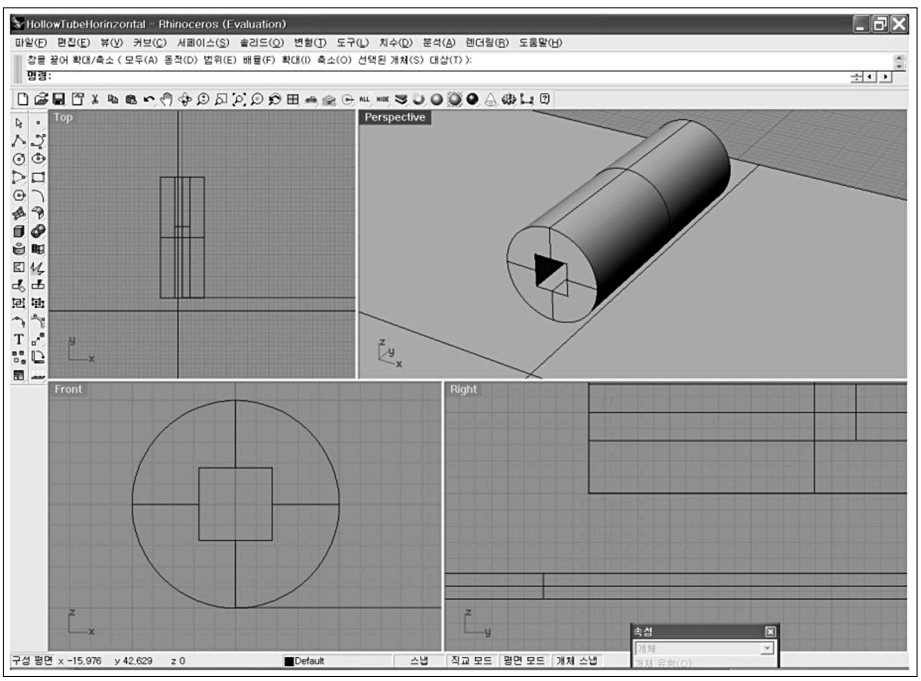

<Fig. 2> A screen shot of the three-dimensional modeling of a virtual hollow filament

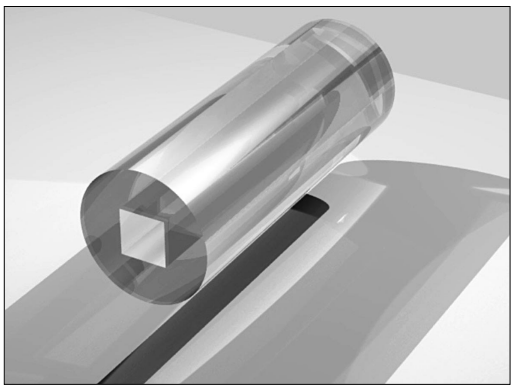

<Fig. 3a> Raytraced image of a hollow nylon filament model with the photon mapping procedure (POV-Ray, two point lights)

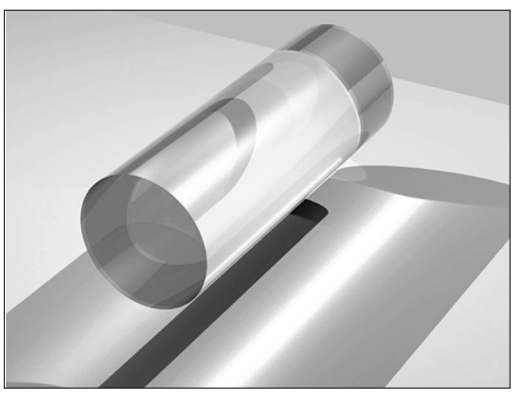

<Fig. 3b> Raytraced image of a regular nylon filament model with the photon mapping procedure (POV-Ray, two point lights)

stacked together parallel to each other, as in the actual yarn or filament fabric, the caustics would form on the surface of the other fibers leading to the higher reflection intensity.

<Fig. 4> shows the images of the actual nylon 6 fabrics. The dyeing procedures for the actual fabrics were different from each other. Therefore, the fabric color shades are different. In <Table 2>, the color depth values are represented by the 'Average of Histogram of the Image Pixel Values'. On the scale of 1 to 65,535, the average value of

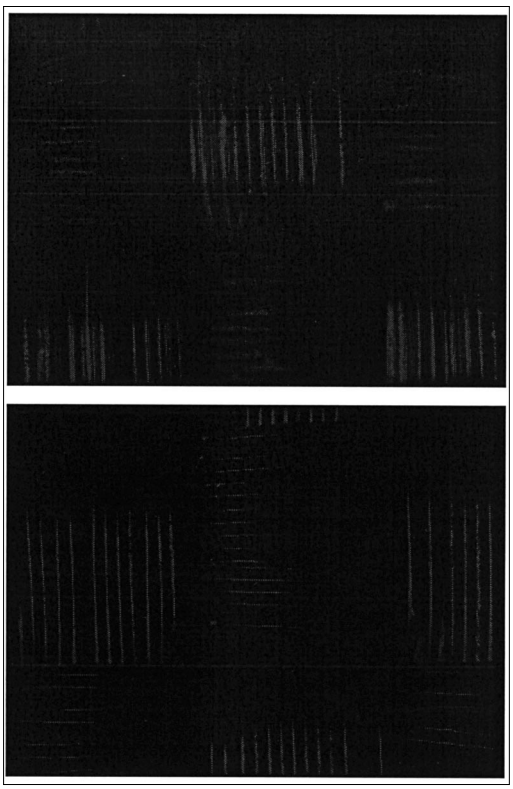

<Fig. 4> Photomicrographs of the actual hollow filament yarn fabric (upper) and regular filament yarn fabric (lower)

the hollow filament fabric is 21,619, and that of the regular filament fabric is 10,638, meaning the shade of the regular filament fabric is darker. It is clear, by visual observation, from the figure that the overall length of the luster objects on the hollow filament yarns is shorter and the luster intensity is subdued compared to those on the regular filament yarns, which are longer and well-defined.

After taking images, the histogram of the image pixel values was constructed, and the average value of the histogram, and the luster objects were analyzed as shown in <Table 2>.

The number of luster objects on the hollow

<Table 2> Image analysis results of the luster objects on the fabric specimens

Item	Hollow Filament Fabric	Regular Filament Fabric
Number of the Luster Objects	43	44
Average Size of the Area of Luster Objects, pixels	1,349.7	2,626.5
Sum of the Area of Luster Objects	58,035	115,565
Average of Histogram of the Image Pixel Values	21,619	10,638

filament fabric was 43, while that of the regular filament fabric was 44. However, the average size of the area of the luster objects of the hollow filament fabric, 1,349.7, is much smaller than that of regular filament fabric, 2,626.5. This indicates that the average luster object of the regular filament fabric is much larger, or the luster is easily recognizable by the eyes. Total area of the luster objects of the hollow filament fabric is 58,035, which is almost half of that of the regular filament fabric, 115,565. This again explains the luster of the hollow filament fabric is quite subdued compared to that of the regular filament fabric. Considering the general trend that the luster becomes generally high when a fabric is dyed towards lighter shade, the difference in the values of 'Sum of the Area of Luster Objects' for the hollow filament fabric and the regular filament fabric is a manifestation that the luster of the hollow filament fabric is subdued compared to the regular filament fabric. <Fig. 5> shows the outlined luster objects on the hollow filament fabric and those on the regular filament fabric based on the <Fig. 4>.

From the images in <Fig. 4>, a section of single filament that was regarded as being

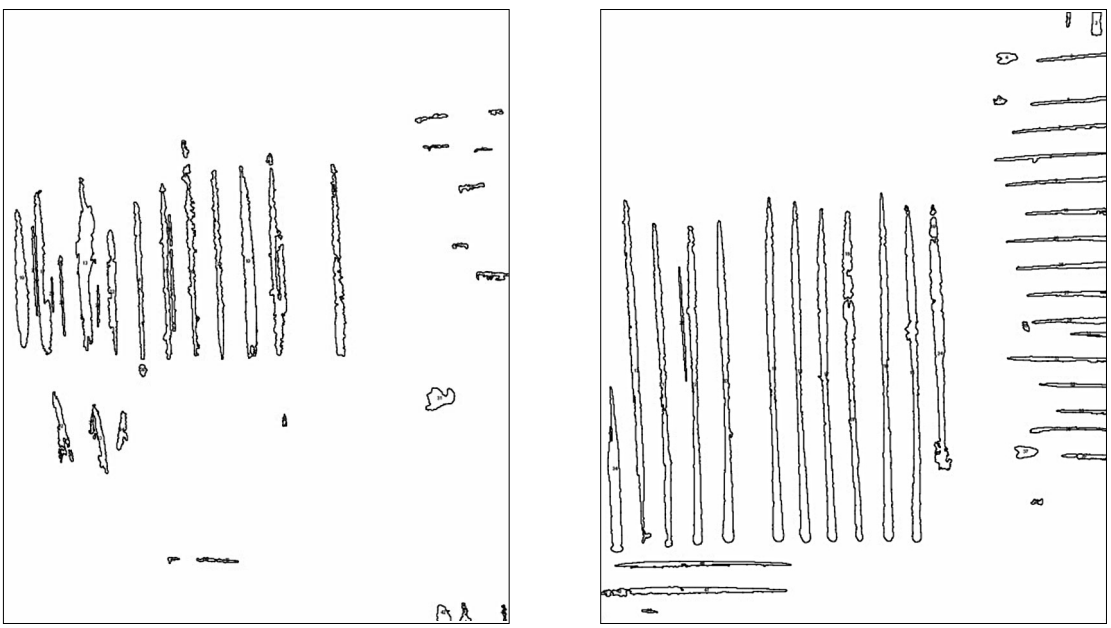

<Fig. 5> Drawing of the outlined luster objects on the hollow filament fabric(left), and the regular fabric(right)

representative of the specimen characteristics well was selected for an image analysis. 'Surface plot' function was applied to the selected rectangular area, 68 by 434 pixels, for comparison of the luster patterns of the filaments. As shown in <Fig. 6a, b>, the pattern of the hollow filament luster image was different from that of the regular filament luster image. The pattern of the hollow filament showed almost two peaks while that of the regular show single well-defined peak. This is probably due to the fact that the hollow filament has square cross-sectional canal, which might also have been further deformed by the subsequent weaving or dyeing process after the melt extrusion, which reflects incident light in a rather complicated pattern compared to the round cross-section regular filament.

V. Conclusions

Hollow continuous filament yarns are being produced to provide advantages such as increased opacity, especially in carpets for hiding dusts or stains, lighter weight fabrics for bags or apparels, better insulation, warmness to the touch, a dry hand which enhances the body and drape characteristics of fabrics made using fine filament yarns. The luster properties of a nylon 6 hollow filament yarn fabric specimen were compared to those of a regular round cross-section filament yarn fabric specimen. In this study, the fabric surface luster image was analyzed using image analysis methods after image acquisition. The hollow filament fiber was modeled using a three-dimensional modeling software. By comparing the virtual luster images

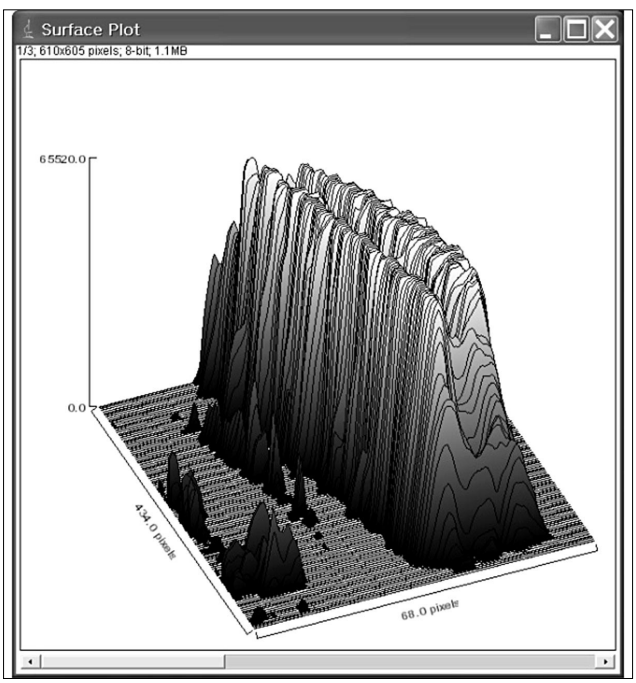

<Fig. 6a> Three-dimensional surface plot of the hollow filament luster

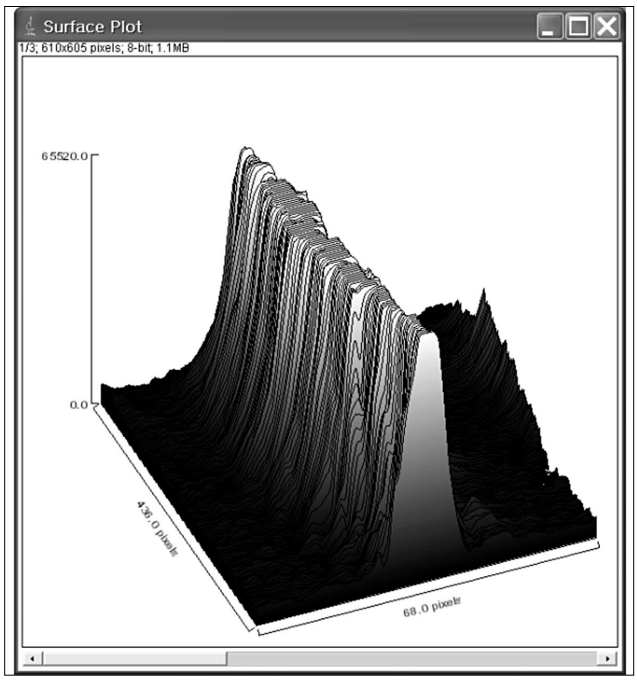

<Fig. 6b> Three-dimensional surface plot of the regular filament luster

of the hollow fiber and the regular fiber models based on shading models including photon mapping, the luster properties of the virtual models were visually different in the surface refection and in the caustics formation on the base plate. The luster objects on the actual hollow nylon 6 filament fabric were smaller than those on the regular filament fabric specimen. The shape of the typical luster object was also different from that of the regular filament fabric; the shape of the hollow fiber luster object was of dual peaks while that of the regular was single peak leading to the luster subtleness difference.

Acknowledgement

The authors would like to express their sincere appreciation to Prof. H. J. Shim, Soongsil University, for his kind supply of the fabric specimens for this study.

References

1. US Pat. 5,532,060, (1996). Continuous Hollow Filaments, Yarns, and Tows
2. Daubert, K., Lensch, H.P.A., Heidrich, W., and Seidel, H. (2001). Efficient Cloth Modeling and Rendering, *Proc. of the EG Rendering Workshop '01*.
3. S., Adanur and T. Liao, (1998). 3D Modeling of Textile Composite Preforms, *Composites*, Part B: Engineering, 29B, pp. 787-793.
4. National Institutes of Health. (2003). "ImageJ", http://rsb.info.nih.gov
5. Robert McNeel and Associates. (2002). *Rhinoceros3D Instruction Manual*.

6. Grum, F., and Becherer, R. J. (1979). *Optical Radiation Measurements*, vol. 1, Academic Press, NY.
7. Phong, Bui-Tuong. (1975). Illumination for Computer Generated Images, *Comm. of the ACM* 18(6), pp. 311-317.
8. Whitted, T. (1980). An Improved Illumination Model for Shaded Display, *Comm. of the ACM*, 23(6), pp.343-349.
9. Jensen, H. W. (2001). *Realistic Image Synthesis using Photon Mapping*, A.K. Peters Ltd., Natick, MA.

Received 1 September, Accepted 23 September.